

Generative Design Process and Optimization of Geodesic Dome with Variable Frequency

*Original*

Generative Design Process and Optimization of Geodesic Dome with Variable Frequency / Sardone, L.; Rosso, M. M.; Melchiorre, J.; Pellegrino, M.. - STAMPA. - 437:(2024), pp. 289-298. ( 2nd Italian Workshop on Shell and Spatial Structures, IWSS 2023 Torino (Ita) 26 June 2023 through 28 June 2023) [10.1007/978-3-031-44328-2\_30].

*Availability:*

This version is available at: 11583/2984107 since: 2024-06-12T21:36:22Z

*Publisher:*

Springer

*Published*

DOI:10.1007/978-3-031-44328-2\_30

*Terms of use:*

This article is made available under terms and conditions as specified in the corresponding bibliographic description in the repository

*Publisher copyright*

Springer postprint/Author's Accepted Manuscript (book chapters)

This is a post-peer-review, pre-copyedit version of a book chapter published in Shell and Spatial Structures. The final authenticated version is available online at: [http://dx.doi.org/10.1007/978-3-031-44328-2\\_30](http://dx.doi.org/10.1007/978-3-031-44328-2_30)

(Article begins on next page)

# Generative Design Process and Optimization of Geodesic Dome with Variable Frequency

Laura Sardone<sup>1,\*</sup>[0000-0002-0928-0606], Marco Martino Rosso<sup>1</sup>[0000-0002-9098-4132], Jonathan Melchiorre<sup>1</sup>[0000-0002-8721-8365], and Marco Pellegrino<sup>2</sup>

<sup>1</sup> DISEG, Department of Structural, Geotechnical and Building Engineering, Politecnico di Torino, Corso Duca degli Abruzzi, 24, Turin, 10129, Italy.

`laura.sardone@polito.it`, `marco.rosso@polito.it`,  
`jonathan.melchiorre@polito.it`

<sup>2</sup> StruSoft AB, Hyllie Boulevard 53, 215 37 Malmö, Sweden  
`marco.pellegrino@strusoft.com`

\* CORRESPONDING AUTHOR: `laura.sardone@polito.it`

**Abstract.** A geodesic dome is a hemispherical thin-shell structure based on a geodesic polyhedron. The triangular elements of the hemisphere are structurally rigid and distribute the structural stress throughout the structure, making geodesic domes able to withstand heavy loads considering their size. After the first geodesic dome was built in Jena (Germany, 1922) on top of the Zeiss optics company as a projection surface for their planetarium projector, thanks to R. Buckminster Fuller, the geodesic domes have been explored far more thoroughly. As a result of their properties, these structures are used for many purposes: as residential modules, greenhouses, water reservoirs and as expositive pavilions. The present paper focuses on geodesic domes optimization, minimizing the overall volume of the frame structure and its connections. In the optimization phase, the base radius of the dome is considered constant, representing a shape constraint. The frequency variability allows for modification of the frame's number, thus varying the structural topology while acting on the shape of the sections (shape optimization). In the case study, self-weight and asymmetric load actions are considered while including the construction aspects for the assembly of a geodesic dome. The optimization phase involves evolutionary genetic algorithms (EAs) exploiting the results of a Finite Element Analysis (FEA).

**Keywords:** Generative Design, Domes, Structural Optimization, Size Optimization, Steel Structures, Risk Management.

## 1 Introduction

Geodesic domes are unique architectural structures characterized by their curved, spherical, or partially spherical shapes, formed by a network of interconnected triangles or polygons. The concept of geodesic domes was popularized by the architect and engineer, R. Buckminster Fuller, in the mid-20th century (**Fig. 1**). A geodesic dome

consists of a framework constituted by a series of struts or beams intersecting and forming triangular or polygonal panels. The panels distribute the structural stress evenly throughout the structure, making geodesic domes sturdy and capable of withstanding several environmental conditions and loads [1].

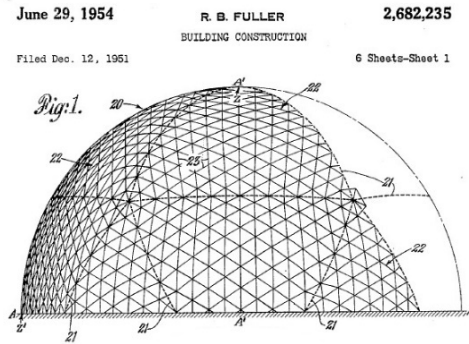


**Fig. 1** Geodesic Dome representation by Fuller Richard Buckminster; Patent US261168A.

The structural integrity of geodesic domes is derived from the inherent strength of triangles. Triangles are inherently rigid and stable, which means that when multiple triangles are interconnected, they create a robust and stable structure. The more triangles incorporated into the dome's design, the stronger and more resilient it becomes [2].

Geodesic domes offer several advantages over traditional architectural forms. Firstly, their spherical or partially spherical shape allows for efficient distribution of stress and load-bearing capacity. This structural efficiency means that geodesic domes require fewer materials compared to conventional buildings of similar size, resulting in reduced construction costs. The unique shape of geodesic domes provides enhanced interior space utilization. With no internal columns or load-bearing walls, the interior can be easily adapted to various purposes, allowing for open and flexible floor plans. Additionally, the curved design of geodesic domes promotes efficient airflow and natural ventilation. These structures have found several applications, ranging from residential dwellings, recreational facilities, greenhouses, exhibition spaces, and even space exploration habitats. Their versatility and adaptability make them popular choices in various industries and contexts [3,4,5,6,7]. Considering the extensive use of geodesic domes in the Architecture, Engineering and Construction (AEC) industry and the continuous studies carried out on this type of structure, in this document the efficiency of geodesic domes is evaluated taking into account the self-weight and the action of the asymmetrical horizontal load (wind action). The FEM analysis is performed through *Alpaca 4D*, a Grasshopper plugin developed on top of *OpenSees*. Finally, a size optimization concerning the geodesic dome's frames is conducted using the meta-heuristic-based Galapagos tool. The results of the structural analyses are then processed through a Python script implemented using the *Iron-Python* component developed in the Grasshopper environment.

## 2 Current implementation of a geodesic dome

### 2.1 Geodesic dome case study description

The geodesic dome under investigation presents a user-defined fixed base radius equal to 10.00m, and it is depicted in **Fig. 2** and **Fig. 3**. The dome was modelled in Grasshopper 3D, a visual programming language and environment that runs within the Rhinoceros 3D computer-aided design (CAD) application (**Fig. 2**) [8].

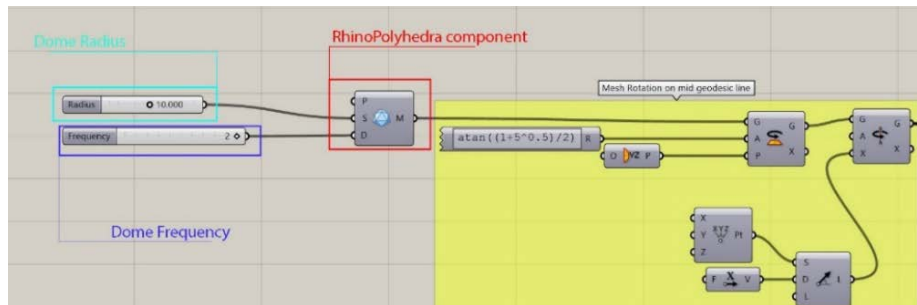


**Fig. 2** Visual Programming environment and Geodesic Dome development with variable radius and frequency.

The spherical dome, implemented through the *RhinoPolyhedra* component, was rotated to find the preferential equatorial plane considering the following rotation angle:

$$\alpha \approx \text{atan}\left(\frac{1 + 5^{0.5}}{2}\right) \approx 58^\circ.2825256 \quad (1)$$

The angle described in Eq.1 permits the initial spherical dome to be rotated in order to obtain the cutting plane detecting the mid-cutting line of the hemisphere (**Fig. 3**).

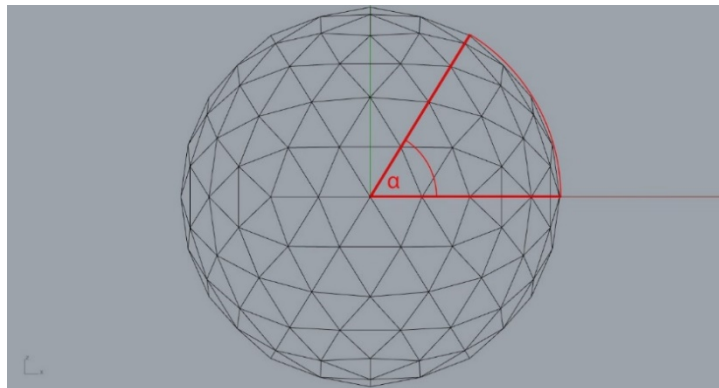


**Fig. 3.** Rotation angle  $\alpha$  representation described by Eq. (1).

## 2.2 Structural analyses and actions

For structural analyses, the open-source plugin Alpaca4D has been adopted. It is based on the well-acknowledged Open System for Earthquake Engineering Simulation (OpenSees) software [9] developed by researchers at the University of California, Berkeley. The finite element (FE) model implements a steel material with grade S355 for the geodesic dome's structure using circular hollow core (CHS) section elements. The boundary conditions of each member are fixed-fixed, and the entire dome presents global support restraints at the base. Two different load cases have been considered, the first one under ultimate limit state (ULS) and the second one under service limit state (SLS) design conditions, see EN 1990 Eurocode 0 "*Basis of structural design*" [10]. Specifically, the latter adopted the SLS characteristic load combination for maximum deformation assessments, i.e., the maximum displacement criterion, as discussed in the next section. The load actions in the structural models are related to the self-weight, automatically computed by the software based on the specific cross-section adopted for each member, a carried permanent load, empirically defined as  $1.00 \text{ kN/m}^2$  of dome's surface accounting for the specific typology of the roofing system (e.g. glass panels and relative connection system to the supporting dome's frames), and a horizontal wind variable action. The wind action has been determined based on the technical procedure of the Italian regulation for structural design NTC2018 [11]. The wind pressure  $p$  is given by

$$p = q_r \cdot c_e \cdot c_p \cdot c_d \quad (2)$$

in which  $q_r$  is the kinetic pressure provided by the well-known Bernoulli theorem from hydraulics engineering  $q_r = \frac{1}{2} \rho v_r^2$ , i.e., depending on the air mass density assumed as  $1.25 \text{ kg/m}^3$ , and the wind reference velocity  $v_r$  of the specific geographical region considered. More precisely, the reference velocity  $v_r = v_b \cdot c_r$  depends on a return coefficient  $c_r$ , set to unity in this case [11], and a reference base velocity  $v_b = v_{b,0} \cdot c_a$ , which in turn depends on an altitude coefficient  $c_a$  and an average base velocity  $v_{b,0}$  measured in 10 minutes, at 10m above plain ground, and with a return period of 50 years, and Since the roofing geodesic dome was hypothetically located in Turin (Italy) at an elevation of  $z = 12\text{m}$  above the ground, thus in an urban area context denoted as Zone 1, the average base velocity is equal to  $v_{b,0} = 25\text{m/s}$ , the altitude coefficient  $c_a$  can be set equal to the unity, determining that the reference velocity  $v_r = 25\text{m/s}$ , and thus a kinetic pressure of  $q_r = 15.625 \text{ N/m}^2$ . Furthermore, the geographical location of the dome and its elevation above the ground determines the value of the exposure coefficient  $c_e$  in Eq. (2), i.e., becoming equal to  $c_e = 1.5$ , thus characterizing an urban environment with a topographic coefficient  $c_t$  equal to unity and a ground roughness of class A [11]. The shape coefficient  $c_p$  depends on the inclination of the roof pitch. The geometry of the geodesic dome imposes considering an equivalent roof pitch with an inclination with respect to the horizontal plane forming an angle greater than  $+60^\circ$ , imposing indeed a shape coefficient equal to  $c_p = +0.8$ . Finally, the dynamic coefficient  $c_d$  is assumed as unity in the absence of more precise indications or specific wind surveys. Therefore, the wind pressure for the dome becomes equal to  $p = 18.75 \text{ N/m}^2$ . Eventually, considering the lateral surface under wind pressure, the wind global action

that affects the dome is approximately equal to  $P = 3 \text{ kN}$ . All the above - considered actions were distributed as acting as point loads in all the dome's nodes.

### 3 Size optimization problem statement

The previously described geodesic dome undergoes an optimization process implemented in Rhinoceros Grasshopper using the meta-heuristic-based Galapagos tool. The size optimization problem has been defined according to the classical truss optimization problems [12,13], in which the reduction of material consumption can be assumed as a reduction of the production costs of the structural part of the dome. The design vector  $\mathbf{x}$  has been encoded with two components, i.e., the external diameter  $\phi_{ext}$  in mm of the CHS adopted cross-section for every dome's member and the thickness  $t$  in mm of every tubular section,

$$\mathbf{x} = [x(1), x(2)]^T = [\phi, t]^T \quad (3)$$

For every component of the design vector, the authors have identified a reasonable interval in which to look for the optimal values, based on the admissible ranges of market availability of standard CHS profiles. Specifically, according to the EN 1993-1-1:2005+AC2:2009 Sections 6.2 & 6.3 (Eurocode standards for steel structures), the reasonable admissible intervals are represented by

$$21.3 \text{ mm} \leq \phi \leq 1219 \text{ mm} \quad (4)$$

$$2.3 \text{ mm} \leq t \leq 60 \text{ mm} \quad (5)$$

Therefore, the constrained size optimization problem statement can be expressed as follows:

$$\min V(\mathbf{x}) = \sum_i A_i(\mathbf{x})L_i \quad (6)$$

$$g_1(\mathbf{x}) = \frac{x(2)}{x(1)} - 1 \leq 0 \quad (7)$$

$$g_2(\mathbf{x}) = \frac{N_{Ed,t}(\mathbf{x})}{N_{Rd,t}(\mathbf{x})} - 1 \leq 0 \quad (8)$$

$$g_3(\mathbf{x}) = \frac{N_{Ed,c}(\mathbf{x})}{N_{Rd,b}(\mathbf{x})} - 1 \leq 0 \quad (9)$$

$$g_4(\mathbf{x}) = \frac{u_{max}}{u_{lim}} - 1 \leq 0 \quad (10)$$

In the previous equations, the  $V(\mathbf{x})$  represents the steel volume of the entire dome, depending on the CHS cross-section  $A_i(\mathbf{x})$  of each  $i$ -th adopted member and its length  $L_i$ . The first constraint  $g_1(\mathbf{x})$  represents a geometrical feasibility condition that imposes that the chosen thickness must be lower than half of the CHS external diameter. The constraints  $g_2(\mathbf{x})$  and  $g_3(\mathbf{x})$  are referred to the respectfulness of the design criteria for ULS conditions for members under acting tensile forces  $N_{Ed,t}(\mathbf{x})$  and acting compression forces  $N_{Ed,c}(\mathbf{x})$ . Specifically,  $g_2(\mathbf{x})$  refers to the allowable tensile strength of each steel member, defined as

$$N_{Rd,t}(\mathbf{x}) = \frac{A_i(\mathbf{x}) \cdot f_y}{\gamma_{M0}} \quad (11)$$

in which  $f_y$  is the steel strength equal to 355 MPa, unless the chosen thickness is greater than 40mm, in this case, the maximum strength is limited to 255 MPa. The coefficient  $\gamma_{M0}$  is the partial safety factor accounting for neglected uncertainties of the semi-probabilistic calculation method, which may be assumed equal to 1.1. On the other hand,  $g_3(\mathbf{x})$  represents the structural assessment of compressed members accounting for possible Eulerian buckling phenomena. Therefore, the compression-resisting value at ULS is defined as

$$N_{Rd,b}(\mathbf{x}) = \chi \frac{A_i(\mathbf{x}) \cdot f_y}{\gamma_{M1}} \quad (12)$$

The reduction factor  $\chi$  may be determined according to the Eurocode 3 formulation, which corresponds to the procedures prescribed in NTC18 [11]. For a hot-rolled CHS profile with steel S355, the instability curve is denoted as “curve a”, which determines an imperfection factor of  $\alpha = 0.21$ . This latter accounts for the existing imperfections of real-world structural members, instead of the classic Eulerian buckling of ideal structural elements. Thereafter, a dimensionless slenderness parameter has to be determined

$$\bar{\lambda} = \sqrt{\frac{f_y \cdot A}{N_{cr}}} \quad (13)$$

which depends on the Eulerian critical buckling compression force

$$N_{cr} = \frac{\pi^2 \cdot E \cdot I(\mathbf{x})}{L_0^2} \quad (14)$$

being  $L_0$  the effective length depending on the boundary conditions of each dome's compressed member. For the sake of conservativeness and for remaining on the safety side, the effective length has been considered equal to the actual length  $L_i$  of each structural element. Finally, the imperfection parameter has been defined as

$$\Phi = \frac{[1 + \alpha \cdot (\bar{\lambda} - 0.2) + \bar{\lambda}^2]}{2} \quad (15)$$

The imperfection parameter has been eventually adopted to define the reduction factor  $\chi$  through the following relation

$$\chi = \frac{1}{\Phi + \sqrt{\Phi^2 - \bar{\lambda}^2}} \quad (16)$$

Eventually, the constraint  $g_4(\mathbf{x})$  expresses the displacement limitation within a reasonable value under the SLS characteristic design condition, expressed in terms of the base radius  $R$  of the geodesic dome.

$$u_{lim} = \frac{1}{250} R \quad (17)$$

The constrained optimization problem stated in Eqs. (6)-(10) has been reformulated as an equivalent unconstrained optimization problem adopting the penalty function method [12,13,14]. Therefore, a new objective function is expressed considering an adaptive penalty term  $\Pi(\mathbf{x})$  [14]:

$$\min \Phi(\mathbf{x}) = V(\mathbf{x})(1 + k_p \cdot \Pi(\mathbf{x})) \quad (18)$$

A penalty factor  $k_p$  has been set equal to  $k_p = 100$  [14]. The penalty term appears as an adaptive term since it will increase the original volume when one or more constraints are violated. Therefore,  $\Pi(x)$  has a value greater than zero when the population individual is unfeasible, and it is zero otherwise:

$$\Pi(x) = \sum_j^4 \max\{g_j(x), 0\} \quad (19)$$

## 4 Results and discussion

The above-mentioned size optimization problem for the geodesic dome was implemented directly in Rhinoceros Grasshopper using the meta-heuristic-based Galapagos tool. Specifically, the structural analyses were conducted with Alpaca4D plug-in both under ULS and SLS conditions. Thereafter, the results of the structural analyses have been collected and processed through a Python script implemented in the Python plug-in of Grasshopper. The script was demanded to determine the objective function (volume) and the penalized volume assessing for the constraints and feasibility of violation. The plug-in Galapagos has been thus connected to the Python script component output, specifically to the penalized objective function, since it works as an unconstrained optimizer tool. The evolutionary solver has been adopted with a population size of 50 individuals. Since different search space topology is defined according to a specific value of the dome's frequency, the authors parametrized the frequency and herein discussed the results of frequency equal to 1 and equal to 2. In the following, the results related to the size optimization problem with the parametrization of the geodesic dome frequencies are presented.

### 4.1 Frequency order 1

The optimization problem was solved by the Galapagos Evolutionary tool in Grasshopper software, and the exact optimal found solution respecting all the constraints after 100 generations for frequency 1 is the following:

$$\mathbf{x}_{opt, frequency=1} = [\phi_{opt}, t_{opt}]^T = [43.7 \text{ mm}, 2.4 \text{ mm}]^T \quad (20)$$

**Fig. 4** shows the 3D representation of the structural model with the optimal values of the design vector. The objective function history during the iterations is illustrated in **Fig. 5** (a), whereas **Fig. 5** (b) shows the bio-diversity ratio. This latter is a percentage value demonstrating that the Evolutionary tool is still exploring the search space, despite the best solution that has been already found in the early generations, leading to a final optimal steel volume of  $0.06 \text{ m}^3$  at the exact design parameters. However, in order to provide a more realistic feasible structural solution, the exact design parameters were rounded up to the closest CHS steel profile already available on the market, according to the EN 1993-1-1:2005+AC2:2009 Sections 6.2 & 6.3. Therefore, the optimal technical solution for size optimization of the geodesic dome under investigation with the

dome's frequency equal to 1 is  $\mathbf{x}_{opt, frequency=1}^* = [\phi_{opt}^*, t_{opt}^*]^T = [48.3 \text{ mm}, 2.6 \text{ mm}]^T$  to which corresponds a slightly higher volume of  $0.073 \text{ m}^3$ .

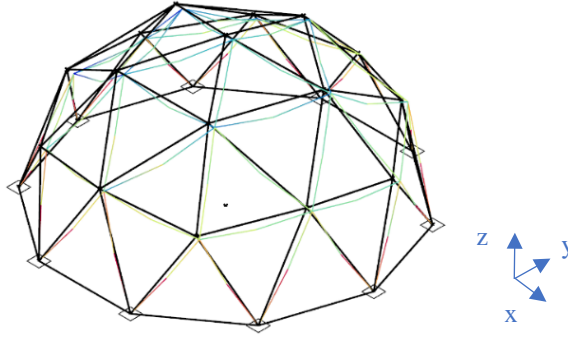


**Fig. 4.** 3D view of the optimal geodesic dome with frequency equal to 1 (black) and the deformed shape (colored).

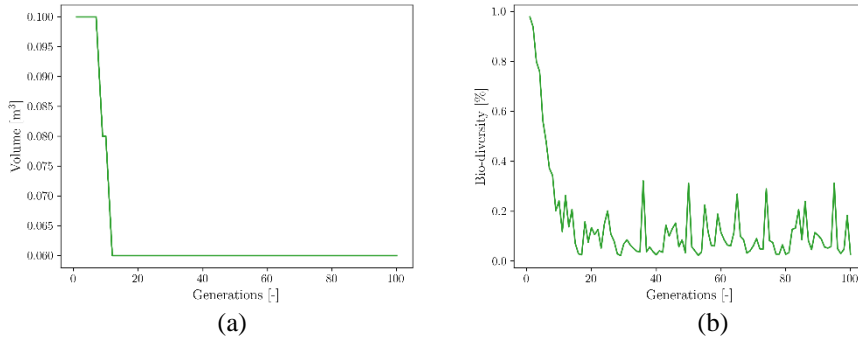


**Fig. 5.** Geodesic dome with frequency 1. (a) Best fitness value of the first element of the sorted population for every explored generation. (b) Bio-diversity ratio during the generations.

## 4.2 Frequency order 2

On the other hand, the optimization process for frequency 2 leads to the following exact optimal solution:

$$\mathbf{x}_{opt, frequency=2} = [\phi_{opt}, t_{opt}]^T = [21.7 \text{ mm}, 3.4 \text{ mm}]^T \quad (21)$$

The above exact solution is respectful of all the imposed constraints, and it is associated with an optimal volume of  $0.08 \text{ m}^3$ . **Fig. 6** shows the 3D representation of the structural model with the optimal values of the design vector. The objective function history during the iterations is illustrated in **Fig. 7** (a), whereas **Fig. 7** (b) shows the bio-diversity ratio. Again, in order to provide a more realistic feasible structural solution, the exact design parameters were rounded up to the closest CHS steel profile already available

on the market, according to the EN 1993-1-1:2005+AC2:2009 Sections 6.2 & 6.3. Therefore, the optimal technical solution for size optimization of the geodesic dome under investigation with the dome's frequency equal to 2 is  $\mathbf{x}_{opt, frequency=2}^* = [\phi_{opt}^*, t_{opt}^*]^T = [26.9 \text{ mm}, 3.2 \text{ mm}]^T$  to which corresponds a slightly higher volume of  $0.095 \text{ m}^3$ . This solution is still respectful of all the imposed constraints.

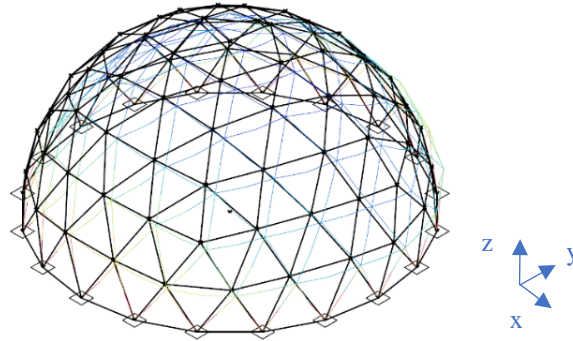


**Fig. 6.** 3D view of the optimal geodesic dome with a frequency equal to 2 (black) and the deformed shape (coloured).

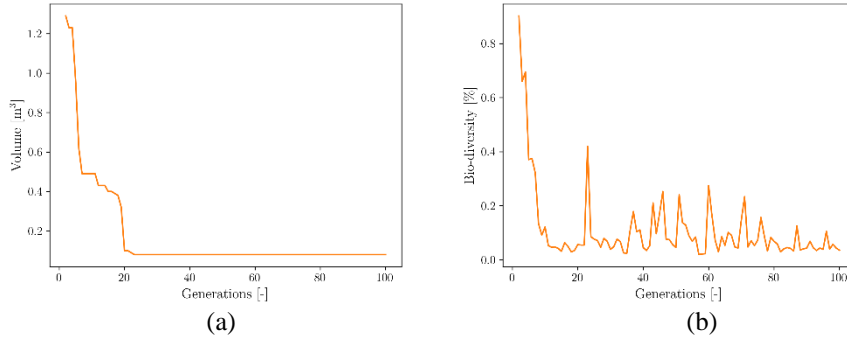


**Fig. 7.** Geodesic dome with frequency 2. (a) Best fitness value of the first element of the sorted population for every explored generation. (b) Bio-diversity ratio during the generations.

## 5 Conclusions

In this document, the efficiency of geodesic domes is evaluated considering the self-weight and the action of the asymmetrical horizontal load (wind action). The FEM analysis is then performed to retrieve the data necessary to achieve the optimal solution evaluating two different dome frequencies. The results show no violations of the imposed constraints while minimising the volume of structure and the computational costs, thanks to the high performance of the produced script. The entire workflow lays

the foundations for a future study that includes seismic actions thanks to the connection between generative design - with the parameterization of geometric data - and OpenSees, used to simulate the performance of structural and geotechnical systems subjected to earthquakes. Although the application was performed on a geodesic dome, the workflow is suitable for several analyses and optimisation implementing different structures comprehending several structural systems.

### Acknowledgement

This work is also part of the collaborative activity developed by Dr Laura Sardone within the framework of the "PNRR": VS3 "Earthquakes and Volcanos".

### References

1. Šiber A. Icosadeltahedral Geometry of Geodesic Domes, Fullerenes and Viruses: A Tutorial on the T-Number. *Symmetry*. 2020; 12(4):556. DOI:10.3390/sym12040556.
2. Rebelo HB, Amarante dos Santos F, Cismaşiu C, Santos D. Exploratory study on geodesic domes under blast loads. *International Journal of Protective Structures*. 2019;10(4):439-456. DOI:10.1177/2041419618820540.
3. Gythiel W., Mommeyer C., Raymaekers T., Schevenels M.; A Comparative Study of the Structural Performance of Different Types of Reticulated Dome Subjected to Distributed Loads, *Frontiers in Built Environment*, Vol.6, 2020. ISSN=2297-3362, DOI: 10.3389/fbuil.2020.00056.
4. Melchiorre, J., et al. "Differential formulation and numerical solution for elastic arches with variable curvature and tapered cross-sections." *European Journal of Mechanics-A/Solids* 97 (2023): 104757.
5. Marano, G. C., M. M. Rosso, and J. Melchiorre. "Optimization as a Tool for Seismic Protection of Structures." *17th World Conference on Seismic Isolation (17WCSI)*. 2023.
6. Sardone, L., et al. "Computational Design of Comparative models and geometrically constrained optimization of a multi-domain variable section beam based on Timoshenko model." *Eurogen2021 proceedings, 14TH Eccomas Conference, Athens, Greece*. 2021.
7. Frangedaki, E., Sardone L., and N. D. Lagaros. "Design optimization of tree-shaped structural systems and sustainable architecture using bamboo and earthen materials." *Journal of Architectural Engineering* 27.4 (2021): 04021033.
8. McNeel, R., & others. (2010). *Rhinoceros 3D, Version 7.0*. Robert McNeel & Associates, Seattle, WA.
9. Mazzoni, Silvia, et al. "OpenSees command language manual." *Pacific Earthquake Engineering Research (PEER) Center* 264.1 (2006): 137-158.
10. EN 1990 (2002) (English): Eurocode - Basis of structural design [Authority: The European Union Per Regulation 305/2011, Directive 98/34/EC, Directive 2004/18/EC]
11. NTC 2018. "DM del Ministero delle Infrastrutture e dei trasporti del 17/01/2018. Aggiornamento delle Norme Tecniche per le Costruzioni (in Italian)." (2018).
12. MacBain, Keith M., and William R. Spillers. *Structural optimization*. Springer US, 2009.
13. Rao, Singiresu S. *Engineering optimization: theory and practice*. John Wiley & Sons, 2019.
14. Rajeev, Srijith, and C. S. Krishnamoorthy. "Discrete optimization of structures using genetic algorithms." *Journal of structural engineering* 118.5 (1992): 1233-1250.